THE JOURNAL OF PHYSICAL CHEMISTRY B

Article

pubs.acs.org/JPCB

Replication Protein A Unfolds G-Quadruplex Structures with Varying Degrees of Efficiency

Mohammad H. Qureshi,[†,‡] Sujay Ray,[‡,§] Abby L. Sewell,[∥] Soumitra Basu,[∥] and Hamza Balci*[,§]

[§]Department of Physics, [†]Department of Biological Sciences, and [∥]Department of Chemistry and Biochemistry, Kent State University, Kent, Ohio 44242, United States

Supporting Information

ABSTRACT: Replication protein A (RPA) is known to interact with guanine- (G-) rich sequences that adopt G-quadruplex (GQ) structures. Most studies reported in the literature were performed on GQ formed by homogeneous sequences, such as the human telomeric repeat, and RPA's ability to unfold GQ structures of differing stability is not known. We compared the thermal stability of three potential GQ-forming DNA sequences (PQSs) to their stability against RPA-mediated unfolding using single-molecule fluorescence resonance energy transfer (FRET) and bulk biophysical and biochemical experiments. One of these sequences is the human telomeric repeat and the other two, located in the promoter region of tyrosine hydroxylase gene, are highly heterogeneous sequences that better represent PQSs in the genome. The three GQ constructs have thermal stabilities that differ significantly. Our measurements showed that the most thermally stable structure (T_m = 86 °C) was also the most stable against RPA-mediated unfolding, although the least thermally stable structure (T_m = 69 °C) had at least an order-of-magnitude higher stability against RPA-mediated unfolding than the structure with intermediate thermal stability (T_m = 78 °C). The significance of this observation becomes more evident when considered within the context of the cellular environment where protein−DNA interactions can be an important determinant of GQ viability. Considering these results, we conclude that thermal stability is not necessarily an adequate criterion for predicting the physiological viability of GQ structures. Finally, we measured the time it takes for an RPA molecule to unfold a GQ from a fully folded to a fully unfolded conformation using a single-molecule stopped-flow method. All three GQ structures were unfolded within $\Delta t \approx 0.30 \pm 0.10$ s, a surprising result considering that the unfolding time does not correlate with thermal stability or stability against RPA-mediated unfolding. These results suggest that the limiting step in G-quadruplex unfolding by RPA is simply the accessibility of the structure to the RPA protein.

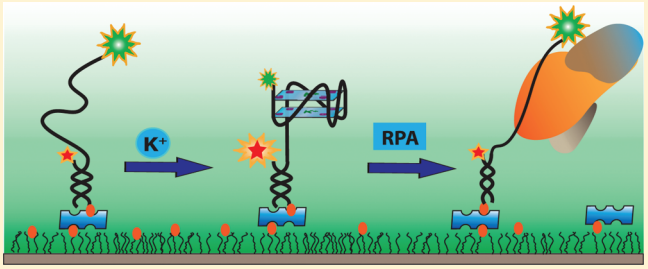

INTRODUCTION

Potential guanine- (G-) quadruplex-forming sequences (PQSs) have been identified in both telomeric and non-telomeric genomic DNA.[1−4] Bioinformatics studies have identified 375000 distinct and nonoverlapping PQSs in the human genome[5] and mapped their distribution.[6−10] Non-telomeric PQSs are overrepresented in or near gene promoters,[9] suggesting that they might be involved in the regulation of gene expression at the transcription level.[11,12] Similarly, RNA G-quadruplexes (GQs) located in the 5′-UTR region[13] have been demonstrated to regulate gene expression at the translational level.[14−16] Recently, the GQs located in the promoter regions of several oncogenes have been targeted by specific small molecules that stabilize the GQ structure in order to modulate gene expression.[17,18]

Despite the abundance of PQSs in eukaryotic genomes and the numerous in vitro demonstrations of such structures, direct demonstration of their existence and function in vivo is challenging.[19] However, recent genome-wide studies have presented indirect but increasingly convincing evidence for the in vivo significance of PQSs. For instance, absence of Pif1, a GQ-unfolding helicase, causes severe retardation in DNA replication and a significant increase in the number of DNA breaks in the GQ-forming segments of the genome.[20] These data were interpreted as evidence for the formation of GQs in vivo and the need for their unfolding by proteins. Because GQs are typically thermodynamically more stable than Watson−Crick base-paired duplex DNA,[21] they would need to be unwound for effective progression of cellular processes that require unwinding of DNA, such as replication and transcription.[19,22] Various helicases, including Pif1, WRN, BLM, and FANC-J, have been shown to perform this task.[22]

Proteins that bind to single-stranded DNA (ssDNA) are also known to unfold GQ structures. Replication protein A (RPA) is the most abundant ssDNA-binding protein in eukaryotes (~1 μM concentration in vivo[23]). RPA has three subunits (RPA70, RPA32, and RPA14) and is involved in DNA replication, repair, and recombination.[24,25] The affinity of RPA for ssDNA ($k_d \approx$

Received: January 17, 2012
Revised: April 11, 2012
Published: April 14, 2012

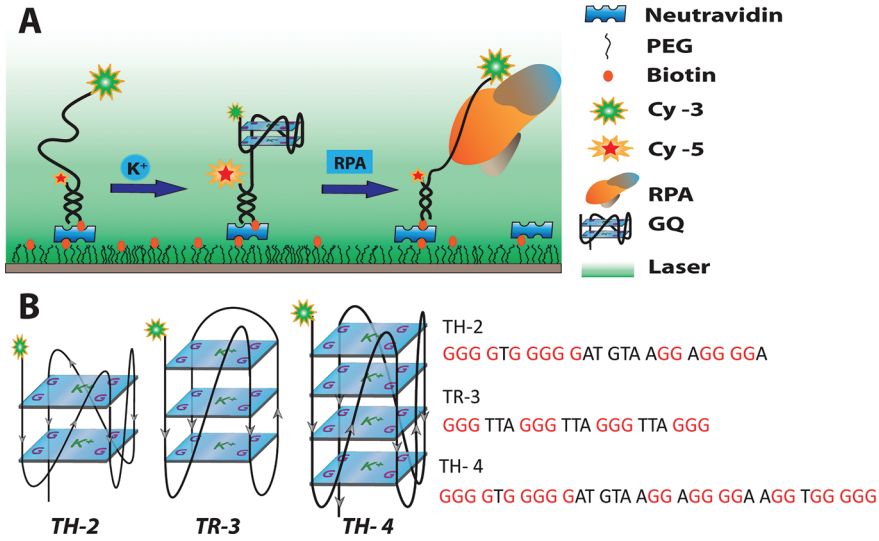

Figure 1. (A) Schematic of single-molecule FRET experiments. GQ-forming DNA constructs are immobilized on a poly(ethylene glycol)-coated quartz slide through a neutravidin−biotin linker. Addition of potassium stabilizes the GQ structure, whereas RPA unfolds the structure. (B) Sequence and a possible folding conformation for each of the three GQ constructs studied in this work. TH-2 and TH-4 are located within the promoter region of the tyrosine hydroxylase gene and can form two- and four-layer GQs, respectively. TR-3 is the human telomeric repeat that forms a three-layer GQ.

10 nM under physiologically relevant conditions) and GQ structures is about 3 orders of magnitude higher than its affinity for double-stranded DNA (dsDNA).[26−28] RPA binding unwinds GQs formed by human telomeric repeat sequence $(TTAGGG)_n$,[26,29−31] and RPA, along with the ssDNA-binding protein Pot1, is known to be involved in telomere maintenance.[32] Interestingly, it has been shown that Cdc13, Stn1, and Ten1, which are proteins specialized for maintaining telomeric DNA, have extensive structural and functional homologies to subunits of RPA.[33,34] It has been proposed that Cdc13, Stn1, and Ten1 form an RPA-like complex that is involved in the maintenance of telomeres. These observations combined with the ubiquitous nature of both RPA and PQSs demonstrate the physiological relevance and significance of RPA−GQ interactions.

In the present study, we compared three GQ constructs in terms of thermal stability and stability against RPA-mediated unfolding. The thermal stabilities of GQs formed by human telomeric and non-telomeric sequences and the RPA-mediated unfolding of GQ formed by human telomeric sequence have been measured.[35,36] However, a comparative study that relates thermal stability and unfolding by RPA of multiple GQ constructs has not been performed. The non-telomeric sequences studied in this work are highly heterogeneous, and the interaction of RPA with such sequences has not been studied before. In particular, the question of whether higher thermal stability also implies higher stability against protein-mediated unfolding has not been addressed. Additionally, the interaction of RPA with any GQ construct, including that formed by human telomeric repeat, has not been studied at the single-molecule level.

METHODS

We used circular dichroism (CD), dimethyl sulfate (DMS) footprinting, and UV thermal melting to characterize the GQs and single-molecule fluorescence resonance energy transfer (FRET) to study RPA−GQ interactions. The experimental methods and protocols followed to perform these measurements are provided in the Supporting Information.

RESULTS AND DISCUSSION

RPA has very high affinity for binding to ssDNA, and the non-tetrad portions (e.g., loops) of GQs can act as natural substrates for RPA. Therefore, we hypothesized that a long loop in the GQ structure could dramatically reduce the stability of the GQ against RPA-mediated unfolding, whereas the effect of such a long loop on thermal stability might not be as significant. The critical step in this process was finding a GQ structure with a relatively high melting temperature as well as a long loop within its structure. Structures with both of these attributes should be difficult to locate, as longer loops have been shown to decrease thermal stability.[35] Identification of a GQ structure with a long loop and high thermal stability motivated us to address this question using a small set of GQ structures.

Such a GQ structure is formed by a non-telomeric and heterogeneous sequence (referred to as TH-2) that forms a two-layer GQ and could potentially include a six- to nine-nucleotide-long loop despite its relatively high melting temperature of T_m = 78 °C. For comparison, we studied two other GQ structures as well: a homogeneous telomeric repeat that forms a three-layer GQ (TR-3) and a heterogeneous non-telomeric construct that potentially forms a four-layer GQ (TH-4). The TH-2 and TH-4 sequences are located within the promoter region of the tyrosine hydroxylase gene.[37] The TH-2 sequence is embedded within the TH-4 sequence, which has an additional segment that enables a four-layer GQ structure. (See Figure 1B for the sequence and a possible folding pattern for each GQ.)

CD measurements were performed to confirm GQ formation in each of the three PQSs at 100 mM K^+ concentration as summarized in Figure 2A. (Control measurements in 100 mM Li^+ are shown in Figure S1 of the Supporting Information.) The CD spectrum of TH-2 exhibits a peak at 260 nm and a trough at 240 nm, which is consistent with parallel GQ conformation. On the other hand, TH-4 has a shoulder around 260 nm in

dx.doi.org/10.1021/jp300546u | J. Phys. Chem. B 2012, 116, 5588−5594

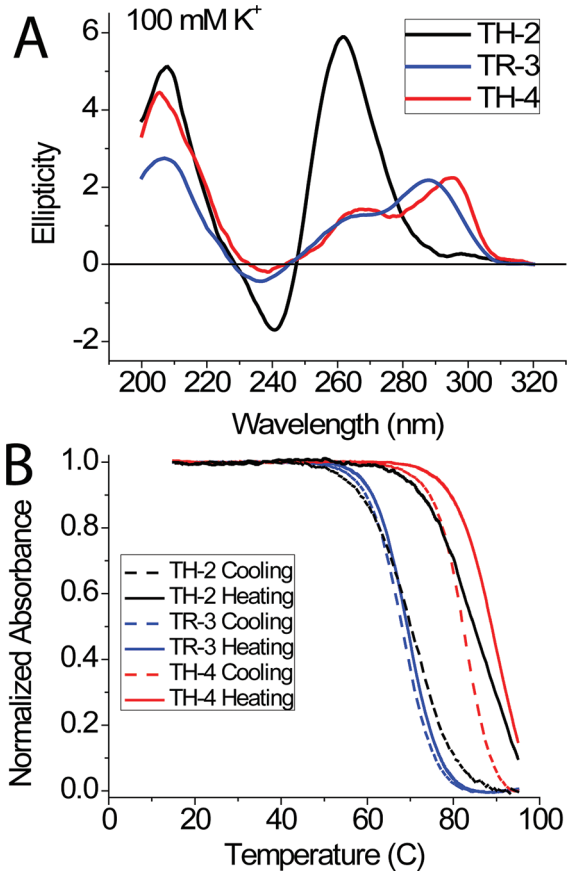

Figure 2. (A) Circular dichroism and (B) UV thermal melting measurements on the three GQs studied in this work. The two types of measurements were performed under conditions similar to those used for single-molecule FRET measurements for consistency. The CD measurements demonstrate GQ formation for all three constructs. The UV thermal melting measurements were used to characterize the thermal stability of the GQ structures.

addition to another peak at 295 nm, suggesting a mix of parallel and antiparallel GQs or a hybrid conformation. The spectrum of TR-3 is similar to that of TH-4, with the exception of the second peak being at 288 nm rather than 295 nm, consistent with a hybrid conformation.[38,39] It should be mentioned that CD data are used to provide evidence of GQ formation rather than to identify the exact GQ conformation, as there are exceptions to the presented interpretations on conformations.[40] In this study, we focused on comparing the average thermal stability of GQs with the RPA-mediated unfolding activity of such structures. The thermal stabilities of the GQs were determined by UV melting measurements, and the following melting temperatures were obtained: T_m(TH-2) = 78 °C, T_m(TR-3) = 69 °C, and T_m(TH-4) = 86 °C (Figure 2B).

Dimethyl sulfate (DMS) footprinting experiments were performed to distinguish the guanines that are part of the G-tetrad structure, which would protect them from DMS modification, from those that are within the loop regions and are therefore not protected.[41] The results of these measurements are reported in Figure S2 (Supporting Information). Based on the DMS protection pattern, one of the many possible GQ structures is shown for each sequence in Figure 1B. The DMS footprinting data suggest that there is no unique set of guanines that participate in the GQ structure for TH-2 and TH-4. Redundancy in the sequences allows for different subsets of contiguous guanines to participate in GQ formation, resulting in a variety of possible structures.

Single-molecule FRET measurements were performed in prism-type total-internal-reflection configuration, as schematically shown in Figure 1A.[42−44] Proper folding into a GQ structure was monitored by measuring the FRET efficiency between the donor and acceptor fluorophores. Increasing K^+ concentration results in stabilization of the GQ, thereby decreasing the distance between the donor−acceptor fluorophores and resulting in higher FRET efficiency (see Figure S3 in the Supporting Information for K^+ titration data on TH-2). At 100 mM K^+, all three constructs showed a single high FRET peak suggesting stable folding (Figure 3). It should be noted that a single FRET population does not necessarily mean a single GQ folding conformation, as the distances between the donor and acceptor fluorophores could be similar for different conformations. To minimize the interaction between the fluorophores and the GQ structure, thymidine spacers were placed between the fluorophores and GQ (see the Supporting Information for sequences). We confirmed that these spacers did not have a significant effect on the thermal stability of the GQs and that constructs with and without the spacers had similar melting temperatures (data not shown). Finally, single-molecule FRET measurements are performed at picomolar DNA concentrations, thereby excluding possibility of intermolecular GQ formation.

The single-molecule FRET data in Figure 3 summarize the unfolding of the GQs at 100 mM K^+ by different RPA concentrations. Among the three GQs, the stability against RPA-mediated unfolding varied by orders of magnitude. TH-2 was found to be the least stable against RPA and completely unfolded in the presence of about 25 nM RPA. TR-3 and TH-4 demonstrated an unexpected unfolding pattern: Both were significantly unfolded at relatively low RPA concentrations (<100 nM) but maintained steady-state unfolded/folded proportions up to physiological-level RPA concentrations (~1 μM). For TR-3, the steady-state unfolded population constituted about 86% of the total population, whereas for TH-4, it was about 49%. The bottom panels in Figure 3A,B show that the RPA-mediated unfolding activity was fitted well by a Langmuir isotherm of the form $y = x/(x + k_D)$, where y represents the fraction of unfolded GQ structures, x is the concentration of RPA in the solution, and k_D is the dissociation constant. This expression is justified because the surface concentration of GQ (subnanomolar) is much lower than the protein concentration in solution. To account for incomplete unfolding of GQ for TR-3 and TH-4, the equation was multiplied by a normalization constant to give $y = \alpha x/(x + k_D)$, where α essentially describes the saturating unfolded fraction of GQ. It should be mentioned that this equation assumes that binding of RPA to GQ is equivalent to unfolding of GQ. A more complete description would require separating the two processes; however, given the number of data points obtained in this work and the quality of the fits based on the simplified model, we believe that we would not be able to distinguish between the two models. Two parameters were extracted from these fits, namely, α and k_D, which represent the fraction of unfolded GQs at saturation (up to physiological RPA concentration, which is about 1 μM) and the dissociation constant of binding/unfolding process, respectively. The results of the fits are as follows: $y = x/(x + 2.3)$ for TH-2, $y = 0.86x/(x + 8.9)$ for TR-3, and $y = 0.49x/(x + 27)$ for TH-4. These results mean that RPA can bind and unfold all TH-2 molecules

dx.doi.org/10.1021/jp300546u | J. Phys. Chem. B 2012, 116, 5588−5594

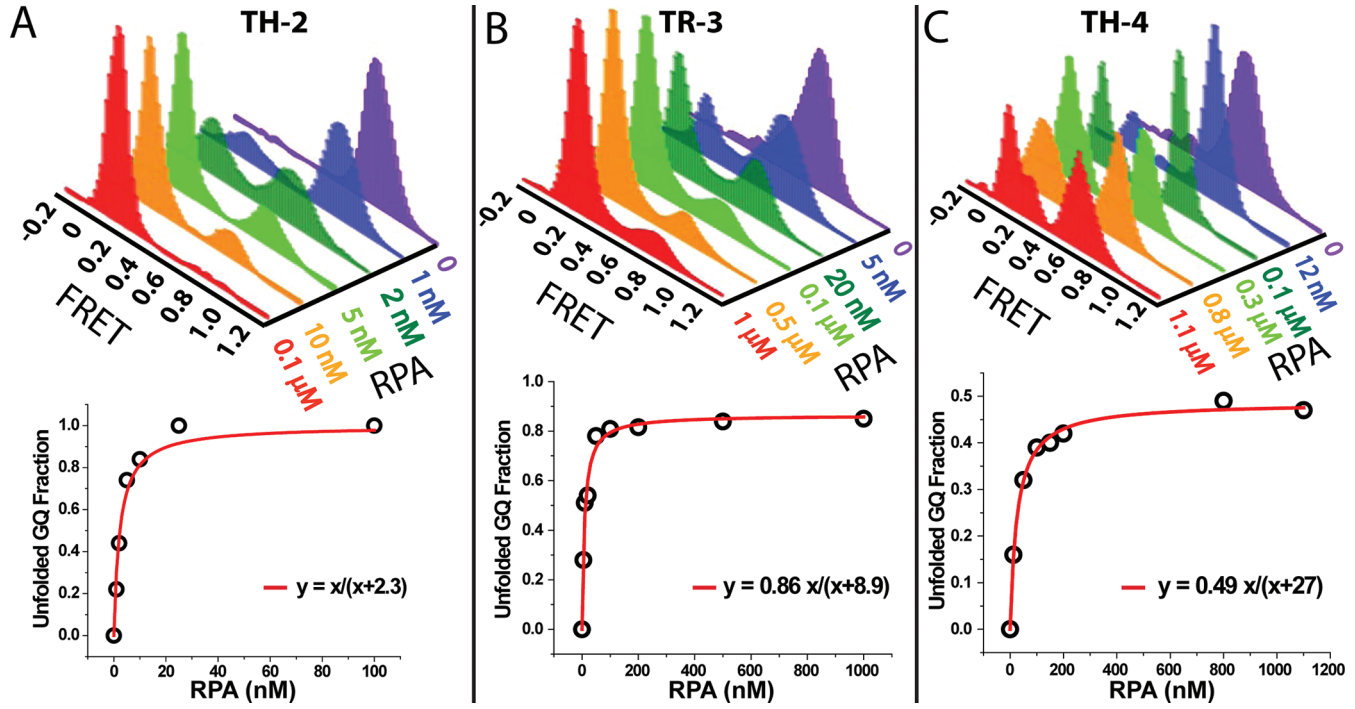

Figure 3. Results of single-molecule FRET experiments probing GQ unfolding at different RPA concentrations for (A) TH-2, (B) TR-3, and (C) TH-4. When GQ is folded, the donor and acceptor dyes are close to each other, resulting in high FRET efficiency. RPA binding to DNA induces GQ unfolding, separating the fluorophores from each other and resulting in low FRET efficiency. As the RPA concentration was increased, the population of the low FRET peak gradually increased as more GQ constructs unfolded. For TR-3 and TH-4, the fractions of unfolded GQ structures saturated at certain values, and complete unfolding of all molecules could not be attained. The panels at the bottom show a Langmuir isotherm fit to the unfolding data.

with a dissociation constant of 2.3 nM. However, in the cases of TR-3 and TH-4, only 86% and 49%, respectively, of the GQ molecules can be unfolded at saturating RPA concentrations. The corresponding dissociation constants are k_D = 8.9 nM for the RPA–TR-3 interaction and k_D = 27 nM for the RPA–TH-4 interaction. Despite its lower thermal melting temperature, TR-3 was found to be significantly more stable against RPA-mediated unfolding than TH-2, as its k_D value was about 4 times higher. In addition, about 14% of the TR-3 molecules were able to maintain a folded structure even in the presence of 1 μM RPA concentration, whereas all of TH-2 molecules were unfolded at less than 100 nM RPA concentration.

The DNA constructs used for this study had a double-stranded stem sequence (see Figure 2), with the donor and acceptor fluorophores placed at the ends of the GQ structure but on separate ssDNA strands. RPA is known to have helix-destabilization activity; however, at near-physiological salt conditions (100 mM KCl and 5 mM $MgCl_2$), the affinity of RPA for dsDNA was measured to be about 3 orders of magnitude smaller than its affinity for ssDNA.[27] It is also known that RPA has indistinguishable affinities for GQ and ssDNA.[26] Furthermore, Fan et al. showed that the affinity of RPA for the duplex formed by a GQ-forming sequence and its complementary strand is negligible compared to its affinity for the GQ-forming sequence alone.[26] Therefore, the possibility of unfolding of the dsDNA stem by RPA can be discarded. All three DNA constructs studied herein had the same dsDNA stem, and therefore, the GQ constructs must be the cause of the significant variation in stability against RPA-mediated unfolding.

Interestingly, the unfolded population of TH-4 exhibited a double peak, with one peak present in the intermediate FRET region, shown in Figure 3C. This suggests that the unfolded state of TH-4 could still maintain some folded secondary structure. RPA has four active DNA-binding domains (DBDs) and can bind an 8–30-nucleotide-long ssDNA.[45] Given that TH-4 is 37 nucleotides long (including the thymidine spacer), it could accommodate an RPA molecule and some folded secondary structure or two RPA molecules at once. If the latter scenario were assumed, the low FRET peak would represent two RPA molecules binding to the same DNA molecule simultaneously. If that were the case, the population of the lower FRET peak would be expected to systematically increase with increasing RPA concentration between 100 nM and 1 μM RPA. However, such a systematic increase was not observed, making this scenario unlikely. The more likely alternative is that the lower FRET peak represents a completely unfolded DNA molecule that is bound by a single RPA molecule. In this case, the intermediate FRET peak would represent an RPA-bound DNA molecule that continued to maintain some folded secondary structure, but not necessarily a GQ.

Finally, we monitored the time required for RPA to unfold GQ using a single-molecule assay resembling the ensemble-level stopped-flow assay. In this assay, we incubated the DNA constructs in a buffer containing 100 mM K^+ for 20 min to attain stably folded GQ structures. Then, we injected a buffer containing 100 mM K^+ and 100 nM RPA while simultaneously recording the data. As a result, we obtained single-molecule FRET time trajectories as shown in Figure 4A, which was acquired at 0.018-s integration time. The initial high FRET state corresponds to the folded GQ conformation, and the following low FRET state corresponds to the RPA-bound unfolded state. By measuring the transition time between these two states, we obtained the time required for RPA to unfold the

dx.doi.org/10.1021/jp300546u | J. Phys. Chem. B 2012, 116, 5588–5594

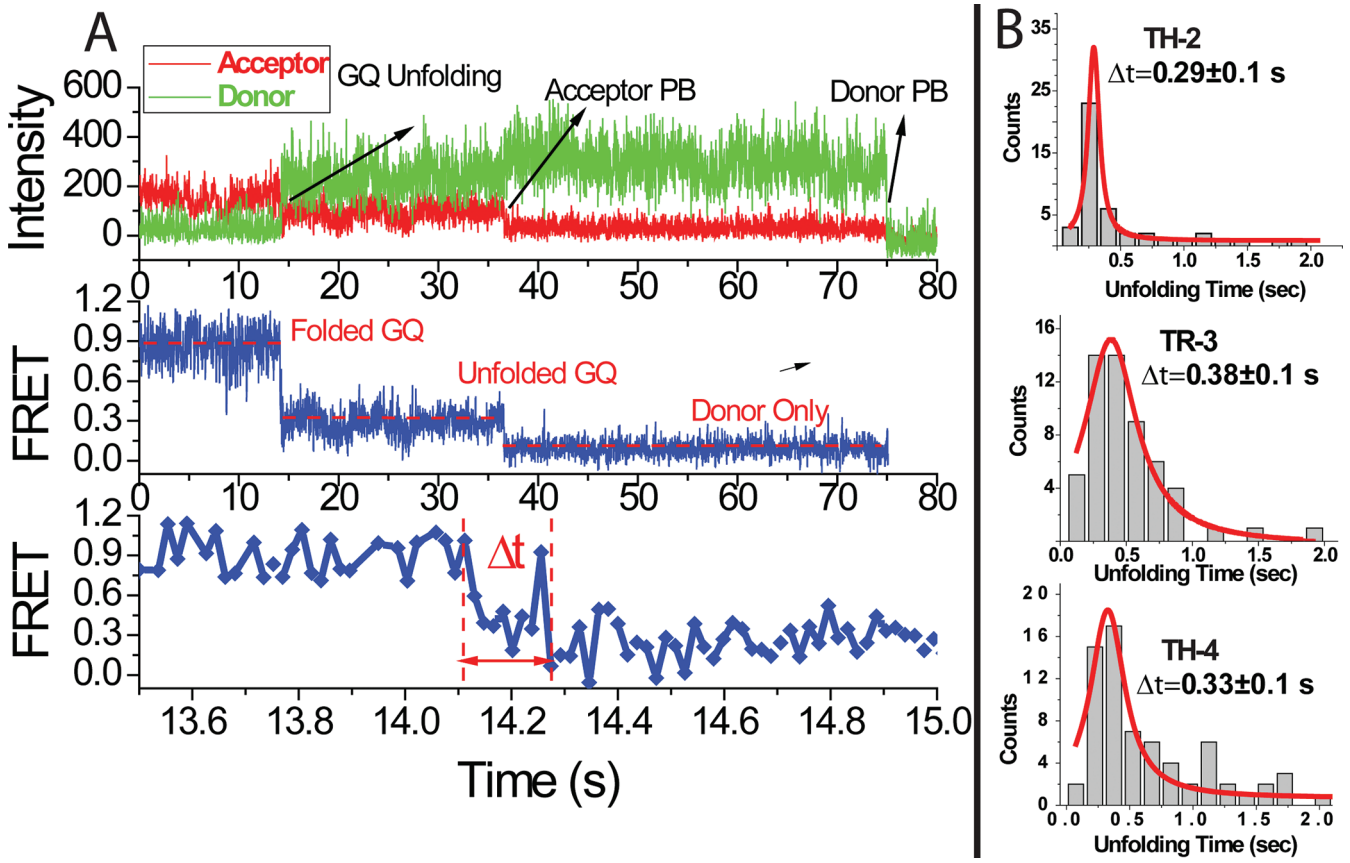

Figure 4. (A) Stopped-flow single-molecule measurements characterizing the unfolding of GQ by RPA. An acquisition time of 0.018 s was used for these data, and the transition from the folded GQ to the unfolded structure upon RPA addition was monitored in real time. GQ unfolding, donor photobleaching (PB), and acceptor photobleaching are indicated in the top graph. Δt represents the unfolding time of GQ by RPA. (B) Histograms of unfolding times obtained using the method described in part A. The histograms were fitted with Lorentzian functions to determine the characteristic GQ unfolding times.

GQ. Several points should be mentioned about this assay to distinguish it from an ensemble-level stopped-flow assay. First, uncertainty in mixing time is not an issue for this single-molecule assay as we monitored the interaction of a single DNA molecule and a single protein molecule in real time. We can determine the exact time, within our time resolution, that a GQ starts unfolding and completes the unfolding process. Hence, the start and end of the unfolding process are determined independently for every GQ molecule included in our analysis. Second, the protein concentration used for the measurements does not affect the transition time. A GQ is unfolded by a single RPA molecule, and the start and end of the GQ unfolding can be determined for each molecule. Having a higher protein concentration would provide a larger number of unfolding events and better statistics. To be consistent, we maintained a 100 nM RPA concentration for all our measurements. Finally, we can distinguish between photobleaching and GQ unfolding and were able to exclude photobleaching events during data analysis. Fluorophore photobleaching could arise because of buffer exchange at the time of RPA flow in the chamber. As shown in Figure 4A, photobleaching and the unfolding transition can be clearly distinguished. Apart from temporal separation between the two events, the FRET level upon GQ unfolding (~0.25) and the FRET level upon acceptor photobleaching (~0.10 for our setup and dye pair) are significantly different and can be easily distinguished. These criteria were applied to all of the data included in the histograms shown in Figure 4B.

The histograms of the unfolding time and Lorentzian fits to these histograms are shown in Figure 4B. During construction of these histograms, the unfolding events that were within a few seconds of RPA injection were used for TH-2 and TH-4, whereas for TR-3, we had to consider later events as well to obtain reasonable statistics. Characteristic unfolding times were determined to be (based on Lorentzian fits) $\Delta t = 0.29 \pm 0.10$ s for TH-2, $\Delta t = 0.38 \pm 0.10$ s for TR-3, and $\Delta t = 0.33 \pm 0.10$ s for TH-4. The image acquisition time for the measurements was 0.035 s, about an order of magnitude smaller than the duration of unfolding transition. We also performed control measurements on the TR-3 construct using a 0.018-s acquisition time, which was achieved by using one-half of the CCD sensor for imaging. An average unfolding time of $\Delta t = 0.27 \pm 0.05$ s was obtained from these measurements (Figure S4, Supporting Information), which is consistent with the data presented in Figure 4 within the uncertainty of the method. The most important contribution to the uncertainty in determining the characteristic times is the uncertainty in selecting the beginning and end of the transition time. We estimate this uncertainty to be about three data points (images), increasing the uncertainty in the measurement to about 0.10 s for a 0.035-s image acquisition time and to about 0.050 s for a 0.018-s image acquisition time. Given this uncertainty, all three GQ structures had essentially the same

dx.doi.org/10.1021/jp300546u | J. Phys. Chem. B 2012, 116, 5588−5594

unfolding time despite significant variations in their melting temperatures and steady-state stabilities against RPA-mediated unfolding. This novel result suggests that the limiting step in the unfolding of GQ structures by RPA is the binding of RPA to GQ. Once RPA binds and the unfolding of GQ starts, it takes similar times for RPA to unfold GQ structures with otherwise very different stabilities. How this binding is influenced by the GQ structure requires systematic studies in which RPA-mediated unfolding is studied with GQ structures with differing loop lengths, sequences, and numbers of G-tetrad layers. Such a systematic study is beyond the scope of the current work, although our results suggest that having a long loop in the GQ structure might be the determining factor in the stability (against protein-mediated unfolding) of certain structures such as the one adopted by TH-2. TH-2 can have a six- to nine-nucleotide loop, depending on which guanines participate in G-tetrad formation. RPA can efficiently bind this loop and destabilize the GQ. In the case of TR-3, the loops are all three nucleotides long, which might be why TR-3 is more stable than TH-2. However, loop length does not describe the entire complexity of the process, as TH-4 has a similar long loop in its structure, 9−10 nucleotides long, but it is very stable against RPA-mediated unfolding. The important difference between TH-2 and TH-4 is, of course, the number of G-tetrad layers: TH-2 has only two tetrad layers, whereas TH-4 has four tetrad layers. Interestingly, the stability against RPA-mediated unfolding was found to correlate with the number of layers; that is, the four-layered TH-4 was found to be the most stable, and the two-layered TH-2 was found to be the least stable. However, understanding how these different structural elements influence the stability of a GQ structure would require systematic studies varying these parameters. However, this study clearly shows that thermal stability alone is not an adequate criterion to determine the stability of a GQ against protein unfolding.

CONCLUSIONS

We have demonstrated that the relative stabilities of GQs against RPA-mediated unfolding can be significantly different from their relative thermal stabilities. Hence, thermal stability alone should not be used as a gauge for putative physiological viability of GQs, given the presence of various unfolding proteins in vivo. It should be emphasized that in vitro RPA−GQ interactions are also not an adequate gauge for in vivo viability, as numerous other molecular factors could affect the stability of a GQ. However, our measurements demonstrate the potential problems that would be encountered if in vivo viability were directly correlated with thermal stability. Potential variables such as the sequence, loop length, and number of G-tetrads could have a dramatically different influence on protein−GQ interactions compared to their influence on the thermal stability of the GQ. In addition, we found the unfolding times of the three GQs by RPA to be very similar, $\Delta t \approx 0.30 \pm 0.10$ s, despite their significantly different melting temperatures. To our knowledge, this quantity has not been measured before, and its similarity between GQ structures with different stabilities suggests that binding of RPA to GQ might be the limiting step in this process. Once RPA binds to GQ, the unfolding event appears to take a place within a very similar time frame for GQs that otherwise have very different stabilities.

ASSOCIATED CONTENT

Supporting Information

Details of experimental procedures, DMS data, control CD experiments in Li^+ solution, data on RPA-mediated unfolding of GQ imaged at 18-ms image integration time, and DNA sequences. This material is available free of charge via the Internet at http://pubs.acs.org.

AUTHOR INFORMATION

Corresponding Author

*Address: Department of Physics, Kent State University, 105 Smith Hall, Kent, OH 44242. Tel.: 330-672-2577. E-mail: hbalci@kent.edu.

Author Contributions

‡These authors contributed equally to this work

Notes

The authors declare no competing financial interest.

ACKNOWLEDGMENTS

We thank Prof. Aziz Sancar and his group members for their help in RPA preparation and Dr. Erdal Toprak for the control UV thermal melting studies. This work was supported by startup funds from KSU to H.B. and S.B. and by NIH Grant 1R15GM096285 to S.B. and H.B. M.H.Q. thanks ICAM for their travel support that enabled RPA purification.

REFERENCES

(1) Blackburn, E. H. *Nature* **1991**, *350*, 569−573.
(2) Gellert, M.; Lipsett, M. N.; Davies, D. R. *Proc. Natl. Acad. Sci. U.S.A.* **1962**, *48*, 2013−2018.
(3) Gilbert, D. E.; Feigon, J. *Curr. Opin. Struct. Biol.* **1999**, *9*, 305−314.
(4) Williamson, J. R. *Annu. Rev. Biophys. Biomol. Struct.* **1994**, *23*, 703−730.
(5) Burge, S.; Parkinson, G. N.; Hazel, P.; Todd, A. K.; Neidle, S. *Nucleic Acids Res.* **2006**, *34*, 5402−5415.
(6) Eddy, J.; Maizels, N. *Nucleic Acids Res.* **2006**, *34*, 3887−3896.
(7) Eddy, J.; Maizels, N. *Nucleic Acids Res.* **2008**, *36*, 1321−1333.
(8) Huppert, J. L.; Balasubramanian, S. *Nucleic Acids Res.* **2005**, *33*, 2908−2916.
(9) Huppert, J. L.; Balasubramanian, S. *Nucleic Acids Res.* **2007**, *35*, 406−413.
(10) Todd, A.; Johnston, M.; Neidle, S. *Nucleic Acids Res.* **2005**, *33*, 2901−2907.
(11) Du, Z.; Zhao, Y.; Li, N. *Genome Res.* **2008**, *18*, 233−241.
(12) Qin, Y.; Hurley, L. H. *Biochimie* **2008**, *90*, 1149−1171.
(13) Huppert, J. L.; Bugaut, A.; Kumari, S.; Balasubramanian, S. *Nucleic Acids Res.* **2008**, *36*, 6260−6268.
(14) Kumari, S.; Bugaut, A.; Huppert, J. L.; Balasubramanian, S. *Nat. Chem. Biol.* **2007**, *3*, 218−221.
(15) Morris, M. J.; Basu, S. *Biochemistry* **2009**, *48*, 5313−5319.
(16) Morris, M. J.; Negishi, Y.; Pazsint, C.; Schonhoft, J. D.; Basu, S. *J. Am. Chem. Soc* **2010**, *132*, 17831−17839.
(17) Balasubramanian, S.; Hurley, L. H.; Neidle, S. *Nat. Rev. Drug Discov.* **2011**, *10*, 261−275.
(18) Balasubramanian, S.; Neidle, S. *Curr. Opin. Chem. Biol.* **2009**, *13*, 345−353.
(19) Lipps, H. J.; Rhodes, D. *Trends Cell Biol.* **2009**, *19*, 414−422.
(20) Paeschke, K.; Capra, J. A.; Zakian, V. A. *Cell* **2011**, *145*, 678−691.
(21) Kumar, N.; Sahoo, B.; Varun, K. A.; Maiti, S. *Nucleic Acids Res.* **2008**, *36*, 4433−4442.
(22) Paeschke, K.; McDonald, K. R.; Zakian, V. A. *FEBS Lett.* **2010**, *584*, 3760−3772.
(23) Kim, C.; Wold, M. S. *Biochemistry* **1995**, *34*, 2058−2064.

(24) Oakley, G. G.; Patrick, S. M. *Front Biosci.* **2010**, *15*, 883−900.
(25) Wold, M. S. *Annu. Rev. Biochem.* **1997**, *66*, 61−92.
(26) Fan, J. H.; Bochkareva, E.; Bochkarev, A.; Gray, D. M. *Biochemistry* **2009**, *48*, 1099−1111.
(27) Lao, Y.; Lee, C. G.; Wold, M. S. *Biochemistry* **1999**, *38*, 3974−3984.
(28) Walther, A. P.; Gomes, X. V.; Lao, Y.; Lee, C. G.; Wold, M. S. *Biochemistry* **1999**, *38*, 3963−3973.
(29) Masuda-Sasa, T.; Polaczek, P.; Peng, X. P.; Chen, L.; Campbell, J. L. *J. Biol. Chem.* **2008**, *283*, 24359−24373.
(30) Salas, T. R.; Petruseva, I.; Lavrik, O.; Bourdoncle, A.; Mergny, J. L.; Favre, A.; Saintome, C. *Nucleic Acids Res.* **2006**, *34*, 4857−4865.
(31) Prakash, A.; Kieken, F.; Marky, L. A.; Borgstahl, G. E. *J. Nucleic Acids* **2011**, 529828.
(32) Flynn, R. L.; Centore, R. C.; O'Sullivan, R. J.; Rai, R.; Tse, A.; Songyang, Z.; Chang, S.; Karlseder, J.; Zou, L. *Nature* **2011**, *471*, 532−536.
(33) Gao, H.; Cervantes, R. B.; Mandell, E. K.; Otero, J. H.; Lundblad, V. *Nat. Struct. Mol. Biol.* **2007**, *14*, 208−214.
(34) Gelinas, A. D.; Paschini, M.; Reyes, F. E.; Heroux, A.; Batey, R. T.; Lundblad, V.; Wuttke, D. S. *Proc. Natl. Acad. Sci. U.S.A.* **2009**, *106*, 19298−19303.
(35) Guedin, A.; Gros, J.; Alberti, P.; Mergny, J. L. *Nucleic Acids Res.* **2010**, *38*, 7858−7868.
(36) Tran, P. L.; Mergny, J. L.; Alberti, P. *Nucleic Acids Res.* **2010**, *39*, 3282−3294.
(37) Romano, G.; Suon, S.; Jin, H.; Donaldson, A. E.; Iacovitti, L. *J. Cell Physiol.* **2005**, *204*, 666−677.
(38) Ambrus, A.; Chen, D.; Dai, J.; Bialis, T.; Jones, R. A.; Yang, D. *Nucleic Acids Res.* **2006**, *34*, 2723−2735.
(39) Phan, A. T. *FEBS J.* **2009**, *277*, 1107−1117.
(40) Masiero, S.; Trotta, R.; Pieraccini, S.; De Tito, S.; Perone, R.; Randazzo, A.; Spada, G. P. *Org. Biomol. Chem.* **2010**, *8*, 2683−2692.
(41) Sun, D.; Hurley, L. H. *Methods Mol. Biol.* **2010**, *608*, 65−79.
(42) Jena, P. V.; Shirude, P. S.; Okumus, B.; Laxmi-Reddy, K.; Godde, F.; Huc, I.; Balasubramanian, S.; Ha, T. *J. Am. Chem. Soc.* **2009**, *131*, 12522−12523.
(43) Lee, J. Y.; Okumus, B.; Kim, D. S.; Ha, T. *Proc. Natl. Acad. Sci. U.S.A.* **2005**, *102*, 18938−18943.
(44) Okumus, B.; Ha, T. *Methods Mol. Biol.* **2010**, *608*, 81−96.
(45) Cai, L.; Roginskaya, M.; Qu, Y.; Yang, Z.; Xu, Y.; Zou, Y. *Biochemistry* **2007**, *46*, 8226−8233.